Master's Thesis

Interaction of MCU with Miro1 Regulates Mitochondrial Functions in Neurons

Ki Do Hong

Department of Biological Sciences

Graduate School of UNIST

2020

Interaction of MCU with Miro1 Regulates Mitochondrial Functions in Neurons

Ki Do Hong

Department of Biological Sciences

Graduate School of UNIST

Interaction of MCU with Miro1 Regulates Mitochondrial Functions in Neurons

A thesis/dissertation
submitted to the Graduate School of UNIST
in partial fulfillment of the
requirements for the degree of
Master of Science

Ki Do Hong

06/04/2020 of submission
Approved by

_____

Advisor
Kyung Tai Min

Interaction of MCU with Miro1 Regulates Mitochondrial Functions in Neurons

Ki-do Hong

This certifies that the thesis/dissertation of Ki-do Hong is approved.

06/04/2020

_____

Advisor: Kyung Tai Min

_____

Professor: Byoung Heon Kang

_____

Professor: Chan Young Park

Abstract

Mitochondrial calcium (Ca^{2+}) uptake is critical for regulating energy metabolism and mitochondrial movement, as well as buffering of intracellular Ca^{2+}. This Ca^{2+} uptake is mediated by a highly selective Ca^{2+} pore complex composed of mitochondrial calcium uniporter (MCU), the inner mitochondrial membrane protein, and its regulatory proteins. Although the mechanism how MCU and its regulatory components regulate mitochondrial Ca^{2+} uptake is well established, a mechanism underlying the regulation of mitochondrial movement by MCU still remain unrevealed. Our previous work found mitochondrial Ca^{2+} content mediated by MCU is a critical factor for regulating the mitochondrial mobility in axon. Here, we find MCU interacts with mitochondrial Rho GTPase 1 (Miro1), known to regulate the mitochondrial mobility. We identify MCU's N-terminal domain, previously known as mitochondrial targeting sequence (MTS), is essential for interaction with Miro1. Our results reveal N-terminus of MCU contains a potential transmembrane domain that makes it possible to interact with Miro1, however, is not required for the localization of MCU into mitochondria. Furthermore, our data shows the elevation of intracellular Ca^{2+} triggers the cleavage of N-terminal domain of MCU, altering the interaction with Miro1, and this Ca^{2+}-dependent MCU-Miro1 interaction is necessary to facilitate the axonal mitochondrial mobility. Together, our findings reveal a novel functional relationship between Miro1 and MCU as a new component of the MCU complex, and a new regulator of mitochondrial movement, respectively.

Contents

List of Figures

Abbreviations

Adenosine triphosphate (ATP)

Alzheimer's disease (AD)

Aspartic acid-Isoleucine-Methionine-Glutamic acid (DIME)

Calcium (Ca^{2+})

Central nervous system (CNS)

Coiled coil (CC)

Essential MCU regulator (EMRE)

Human embryonic kidney 293 cells (HEK293 cells)

Huntington's disease (HD)

Inner mitochondrial membrane (IMM)

Intermembrane space (IMS)

Isocitrate dehydrogenase (ICDH)

MCU paralogue (MCUb)

Mitochondrial calcium uniport (MCU)

Mitochondrial calcium uniporter regulator 1 (MCUR1)

Mitochondrial calcium uptake protein 1-2 (MICU1-2)

Mitochondrial Rho GTPase 1 (Miro1)

Mitochondrial targeting sequence (MTS)

Multiple sclerosis (MS)

Neuroblastoma 2A cells (N2A cells)

N-terminal domain (NTD)

Outer mitochondrial membrane (OMM)

Oxidative phosphorylation (OxPhos)

Parkinson's disease (PD)

Pyruvate dehydrogenase (PDH)

Sarco/endoplasmic reticulum (SR/ER)

Schizophrenia (SCZ)

Small hairpin control vector (shCtrl)

Small hairpin MCU knockdown vector (shMCU)

Trafficking kinesin-binding protein 1-2 (TRAK1-2)

Translocase of outer mitochondrial membrane 20 (TOMM20)

Transmembrane (TM)

Tricarboxylic acid (TCA)

α-ketoglutarate dehydrogenase (α-KGDH)

I. Introduction

Mitochondrion is an essential organelle for neuronal functions and survival.

Mitochondria, double membrane-bound organelles, are found in almost all types of eukaryotic cell[1]. It plays a vital role in synthesizing the adenosine triphosphate (ATP), known to the molecular unit of intracellular energy current, mainly through oxidative phosphorylation (OxPhos)[2]. In addition to its role as the power plant of the cell, mitochondria have a key role in regulating the intracellular calcium homeostasis[3]. These mitochondrial calcium buffering is critically important for both the mitochondrial metabolic activity and the control of calcium-dependent signaling pathway[4-6]. In the central nervous system (CNS) where a great amount of energy and sophisticated regulation of Ca^{2+} homeostasis are demanded[7], mitochondrial functions are of importance to neurons. In particular, appropriate mitochondrial transport and distribution within two highly polarized compartments, dendrites and axon, are essential for supplying energy to these sites of neurons[8]. As a result, mitochondrial functions are directly linked to neuronal function and health. Also, mitochondrial dysfunctions, involving reductions in ATP synthesis, abnormal mitochondrial dynamics and morphology, and impaired mitochondrial transport, are commonly observed in various neurological diseases, such as Alzheimer's disease (AD), Huntington's disease (HD), Parkinson's disease (PD), Schizophrenia (SCZ), and Multiple sclerosis (MS).[9,10]. Although loss of mitochondrial functions in some of neurological diseases may be a secondary or acquired effect obtained from primary sources, there is no doubt that pathogenesis of neurological disorders is exacerbated by defects in mitochondrial functions.[11]

Mitochondrial Ca^{2+} regulates both mitochondrial energy metabolism and transport in neurons.

Ca^{2+} is a ubiquitous second messenger which regulates a variety of biological processes in all eukaryotic cells[12]. These processes include the control of gene transcription, metabolism, cell mobility, cell growth, and programmed cell death, called apoptosis[12]. In neurons, Ca^{2+} is particularly important for regulating neurotransmitter release and membrane excitability for the synaptic transmission[13,14]. Due to its importance as a signaling molecule, extracellular Ca^{2+} influx across the plasma membrane, and intracellular Ca^{2+} storage/release are actively regulated by a large number of membrane transport proteins and subcellular organelles, involving sarcoplasmic/endoplasmic reticulum (SR/ER) and mitochondria[15]. Although ER is considered to be a main cellular compartment for Ca^{2+} storage and release, mitochondria also play a critical role in modulating intracellular Ca^{2+} as the calcium storage/release organelle[15]. These Ca^{2+} uptake into the mitochondria matrix allows mitochondria to be capable of their functions, involving the mitochondrial energy metabolism, and the mitochondrial movement in neurons[16-18]. The activity of three mitochondrial dehydrogenases, pyruvate dehydrogenase (PDH), α-ketoglutarate dehydrogenase (α-KGDH), and isocitrate dehydrogenase (ICDH) in the tricarboxylic acid (TCA) cycle is stimulated by mitochondrial Ca^{2+}[19]. And our previous study found

mitochondrial Ca^{2+} acts as an internal signal to modulate mitochondrial transport, resulting in the redistribution of mitochondria within axons[20]. Imaging analysis of axonal mitochondria with Ca^{2+} indicator showed the inverse correlation between the speed of mitochondrial movement and the mitochondrial Ca^{2+} content[20]. It suggested mitochondrial Ca^{2+} can be a critical factor which facilitates the energy supply to proper sites by modulating mitochondrial distribution.

Molecular identity and mechanism of MCU complex for mitochondrial Ca^{2+} uptake.

Ca^{2+} uptake into mitochondrial matrix is tightly regulated by the MCU complex, a Ca^{2+}-selective channel, across the inner mitochondrial membrane (IMM)[21,22]. This complex is comprised of MCU, the essential pore-forming subunit, and its regulatory subunits, including MCU paralogue (MCUb), mitochondrial calcium uptake protein 1-2 (MICU1-2), essential MCU regulator (EMRE), and MCU regulator 1 (MCUR1) (Figure 1B)[23]. The core subunit, MCU, is characterized by two TM domains, the DIME motif that is important for MCU activity, and two coiled-coil (CC) domains[23] (Figure 1A). A recent study identified MCU forms a pentameric pore in which the second TM domain forms an inner core hydrophilic pore surrounded by the first TM domain[24]. The DIME motif forms the pore entrance exposed to the intermembrane space (IMS). And CC domains make a contribution to stabilize the pore assembly and structure[24]. MCUb, a paralogue of MCU, acts as its dominant-negative subunit. MCUb forms a hetero-oligomer with MCU, resulting in a decrease in Ca^{2+} uptake into mitochondrial matrix in response to the cytosolic Ca^{2+} elevation[25]. MICU1, as an activator or inhibitor of Ca^{2+} uptake through MCU complex, is found in the IMS[26]. It plays a critical role in preventing Ca^{2+} overload in the mitochondrial matrix. Highly conserved EF hand domain within MICU1 serves as a Ca^{2+}-dependent gate sensor of MCU in response to the cytosolic Ca^{2+}[26]. MICU2, its isoform, also has the conserved EF-hand domain and forms a hetero-dimer with MICU1[27]. MICU2, as the MCU gatekeeper, functions to inhibit the Ca^{2+} uptake into mitochondrial matrix at low cytosolic Ca^{2+}[28]. EMRE, located in the IMM, is a metazoan-specific protein containing a single transmembrane (TM) domain[29]. It acts as a sensor of mitochondrial matrix Ca^{2+}, allowing the MCU complex to inhibit Ca^{2+} uptake under normal condition[29]. EMRE interacts with MICU1 at the IMS, suggesting that EMRE functions cooperatively with MICU1/MICU2 to regulate the MCU activity in response to Ca^{2+} on both side of the IMM[30]. MCUR1 interacts with MCU and EMRE, and is required for the MCU complex assembly as a scaffold factor[31,32].

Miro1 is an important component for regulating mitochondrial transport.

Miro1 contains two GTPase domains, two EF hand Ca^{2+}-binding domain between them, and a C-terminal transmembrane domain for anchoring to the outer mitochondrial membrane (OMM)[33] (Figure 2A). Most part in Miro1 involving GTPase domains, and EF hand domains, is exposed on cytoplasmic side of the OMM[34]. The major function of Miro1 is the transport of mitochondria along microtubule tracts[35]. In particular, Miro1 is critical in a long-distance axon and dendrites of the neuron which

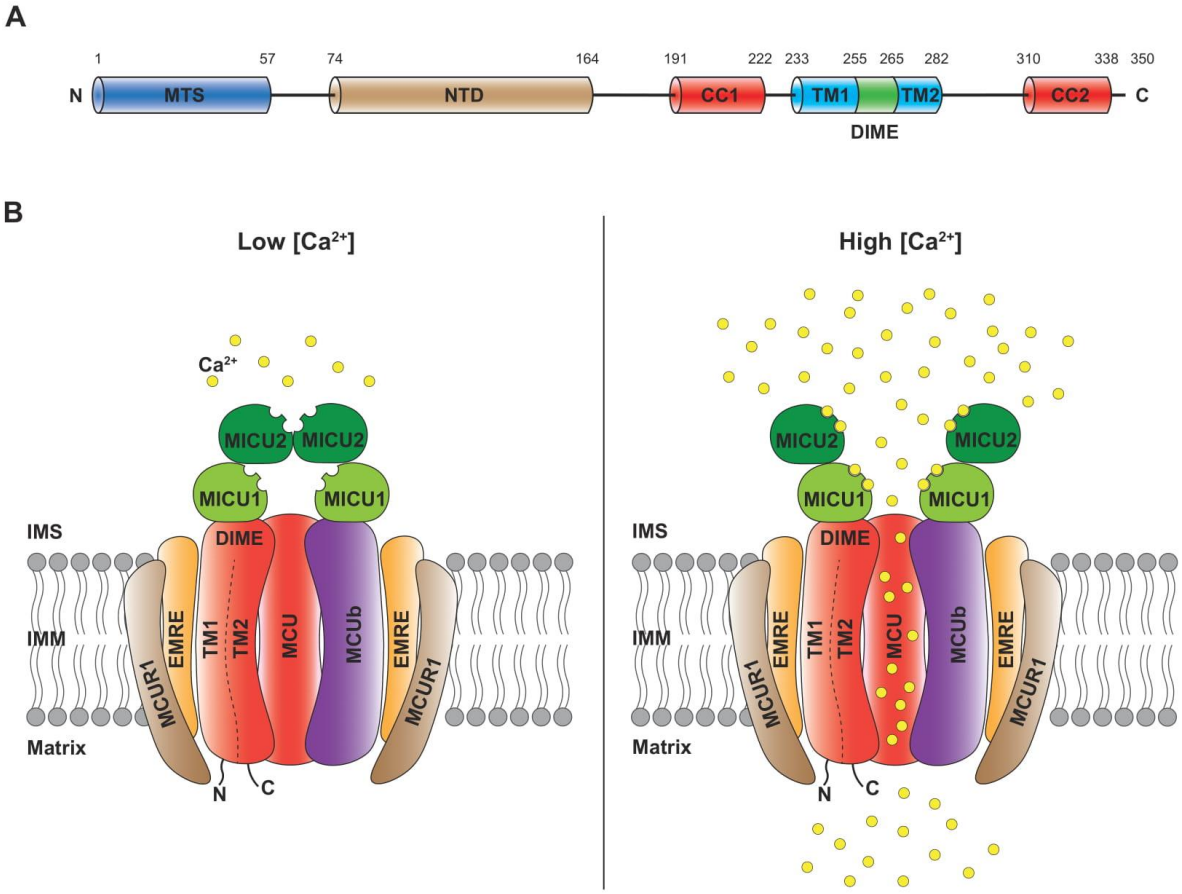

Figure 1. Schematic domain of MCU and molecular structure of MCU complex. (A) Schematic diagram of functional domains of MCU. MCU is composed of putative mitochondrial targeting sequence (MTS), N-terminal domain (NTD), two coiled-coil domains (CC1, CC2), two transmembrane domains (TM1, TM2), and DIME motif flanked by transmembrane domains. (B) Molecular structure of MCU complex. MCU and MCUb as pore-forming subunits form a highly selective Ca^{2+} channel with the regulatory subunits, involving mitochondrial Ca^{2+} uptake protein 1, 2 (MICU1, MICU2), essential mitochondrial Ca^{2+} uniporter regulator (EMRE), and MCU regulator 1 (MCUR1).

requires the efficient mitochondrial transport in response to physiological needs. In a mitochondrial transport machinery, Miro1 binds to the trafficking kinesin-binding protein 1-2 (TRAK1-2)[36]. The Miro1/TRAK complex sequentially interacts with kinesin or dynein motor proteins capable of the anterograde or retrograde mitochondrial movement, respectively[36]. Although the molecular identity and functions of these machinery components are well established, a detail mechanism underlying Ca^{2+}-dependent regulation of the motor/adaptor complex still remains unclear. Up to now, two models of Miro1 in regulating the mitochondrial mobility have been proposed[37]. The first proposed model is that Ca^{2+} binding to EF hands recruits kinesin to mitochondria by directly binding to the Miro1/TRAK

complex, preventing the motor from associating with microtubule tracts[37] (Figure 2B [i]). The second model describes that the conformational change of Miro1 by Ca^{2+} binding to its EF hands allows mitochondria to dissociate from kinesin while TRAK1/2 remains bound to Miro1 with mitochondria[37] (Figure 2B [ii]). Both models indicate mitochondrial movement is arrested by elevated intracellular Ca^{2+} in axon in which Miro1 acts as a Ca^{2+}-dependent mediator through the conformational change upon Ca^{2+} binding to EF hands[37]. Several studies using Miro1 knock-out mouse model showed mitochondrial mobility defects in axons and a motor neuron disease-like phenotype[38,39].

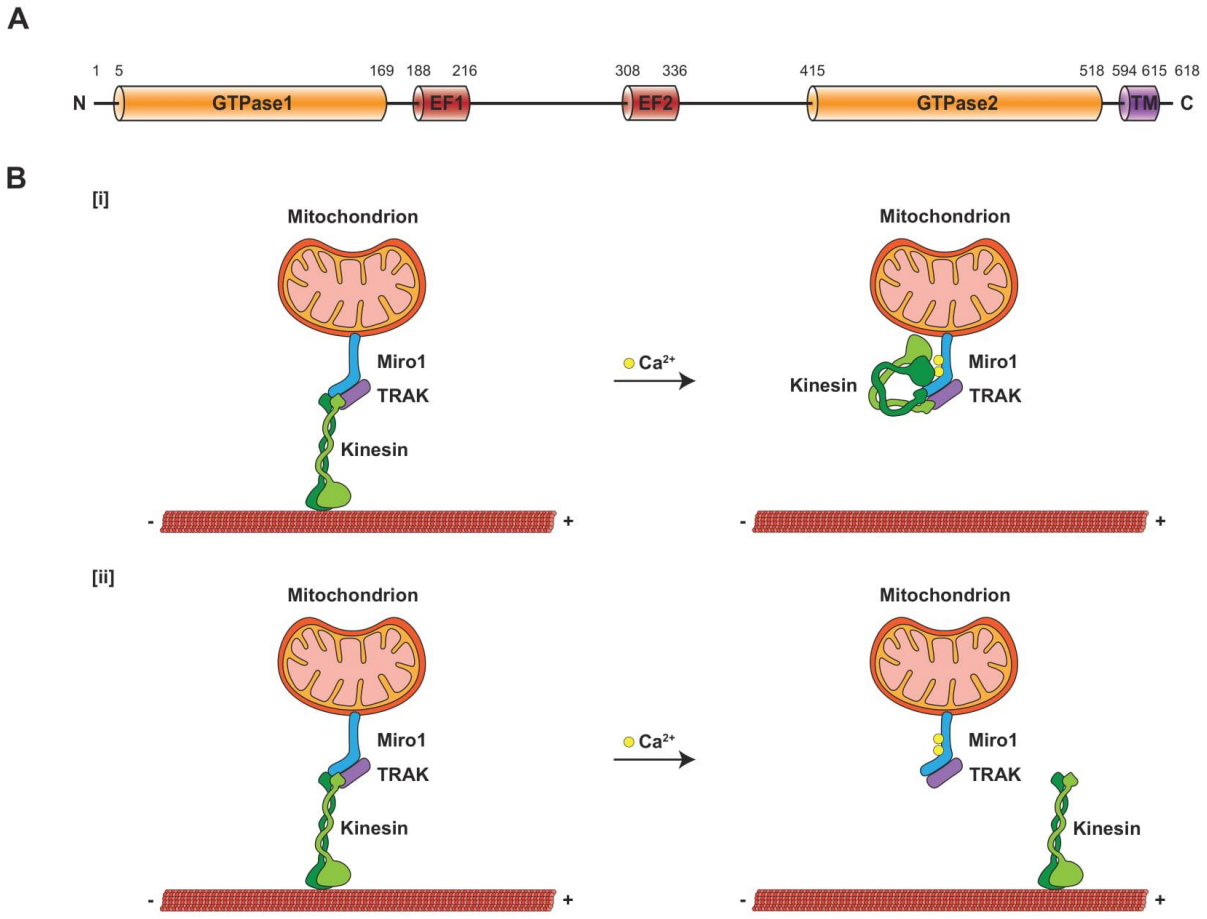

Figure 2. Schematic domain of Miro1 and model of Miro1 in regulating mitochondrial movement. (A) Schematic diagram of functional domains of Miro1. Miro1 is composed of two GTPase domains (GTPase1, GTPase2), two Ca^{2+}-binding EF hands domains (EF1, EF2) flanked by GTPase domains, and a single transmembrane domain (TM) at C-terminus of Miro1. (B) Schematic models of Miro1 in regulating mitochondrial transport. [i] Ca^{2+} binding to Miro1's EF hands triggers the dissociation of the motor protein, kinesin, from mitochondria, leading to detachment of the motor from microtubule tracts. [ii] Ca^{2+} binding to the EF hands allows the kinesin to dissociate from Miro1, while the Miro1/TRAK complex still maintains the binding to mitochondria.

II. Materials and Methods

Animal Care. Animals were used in accordance with protocols approved by the Animal Care and Use Committees of UNIST. C57BL/6 mice were purchased from Hyochang Science (Korea).

Coverslip Preparation. For microscopy experiments, glass bottom dishes (Cellvis, D35-14-1.5-N) and #1.5H coverslips (Deckglaser, ref 0117520) were immersed in 1M HCl for at least 4 hours at 55°C. Next, dishes were washed with autoclaved dH_2O, followed by 50%, 70%, and 100% EtOH for 30 minutes. After washing, dishes were dried in a biological safety cabinet with UV exposure for sterilization. Dried dishes were then coated with 1× PBS containing 50μg/ml of Poly-D-lysine (PDL, Thermo Fisher Scientific, P6407) in cell culture incubator overnight. PDL-coated dishes were washed three times with autoclaved dH_2O, and dried in a biological safety cabinet. PDL-Coated dishes were stored in a cell culture incubator until use.

Plasmid Preparation. shMCU vector was purchased from Sigma-Aldrich (shMCU: TRCN0000251261). Myc-Miro1 plasmid vector was obtained from Dr. Pontus Aspenstrom. MCU was cloned into pFLAG-CMV6B vector (Sigma-Aldrich) using primers 5'CTGAATTCATATGGCGGCCG CCGCAGGTAG3', and 5'GCTGGATCCTCATTCCTTTTCTCCGATCTG3'. C-Flag vector (Addgene, 20011) and sfGFP-N1 vector (Addgene, 54737) were then used for MCU subcloning. TOMM20-Myc was cloned from TOMM20-sfGFP vector, which was subcloned from mEos3.2-TOMM20-N-10 vector (Addgene, 57483). sfGFP was replaced to Myc-tag using the primers 5'TCCGAGGAGGACCTGACC GGTGCGGCCGCGACTCTAGATCA3', and 5'GATCAGCTTCTGCTCAGGATCCCCGCTACCGC CTTCCACATC3'.

Cell Culture. E18 mouse embryos were used in all primary neuron culture. Pregnant mice euthanized in a CO_2 Chamber were sacrificed by cervical dislocation. Embryos were immediately placed on a plate containing ice-cold HBSS (Thermo Fisher Scientific, 14065056). Hippocampi were isolated from embryonic brain, and washed twice with ice-cold HBSS (w/o Ca^{2+} and Mg^{2+}). Trypsin without EDTA (Thermo Fisher Scientific, 15050065) was then added to hippocampi, and incubated for 15 minutes in a 37°C water bath. Next then, hippocampi were immediately transported into a tube containing FBS (Millipore, CAT# TMS-013-BKR) for inactivating trypsin, and washed twice with a trituration media, followed by pipetting up and down gently to cell dissociation. The dissociated cells filtered by 40μm cell strainer (Falcon, ref 352340) was then plated on PDL-coated coverslips or glass bottom dishes at a density of 0.035×10^6 cells/cm^2. 3 hours after cell seeding, the trituration media was exchanged with a neuronal culture media composed of Neurobasal media (Thermo Fisher Scientific, 21103049), B27 (Thermo Fisher Scientific, 17504044), and GlutaMAX (Thermo Fisher Scientific, 35050061). DMEM (Invitrogen) supplemented with 10% FBS and Penicillin/Streptomycin (Thermo Fisher Scientific, 15070063) was used for maintaining HEK293 cells and N2A cells. For transfection into primary neurons, 1μl of Lipofectamine 2000 (Invitrogen) and 1.2μg of plasmid DNA were used with 100μl of

Opti-MEM. Lipofectamine 2000/DNA complexes were incubated for 20 minutes at room temperature. After then, half of the cell culture media was exchanged with the transfection media containing Lipofectamine 2000/DNA complexes. 3hour after transfection, the transfection media was replaced by a 50% mixture of old and fresh cell culture media. For cell lines, 2μl of Lipofectamine 2000 and 2μg of plasmid DNA were used with 200μl of Opti-MEM. Lipofectamine 2000/DNA complexes were incubated for 20 minutes at room temperature, and added to cell culture plates. There was no washout step after transfection.

Mitochondrial Extraction. HEK293 cells were used for extracting mitochondria. First, cells were harvested by incubation into trypsin-EDTA for 5 minutes and centrifugation at 500×g at 4°C. Cell pellets were then washed twice with 1ml of 1×PBS, followed by resuspension in 1ml of ice-cold mitochondrial isolation buffer composed of 200mM Mannitol, 70mM Sucrose, 10mM HEPES pH7.4, 1mM EGTA, and protease inhibitor cocktail. Cells were ruptured by 50-60 strokes with a douncer gently to avoid mitochondrial damage, and centrifuged twice at 700×g at 4°C. The pellet was removed, and supernatant containing intact mitochondria was centrifuged for 10 minutes at 10,000×g at 4°C to obtain purer mitochondrial fraction. For immunostaining of isolated mitochondria, mitochondrial pellet re-suspended in 100μL of the isolation buffer was placed on coverslips. For Proteinase K experiments, the mitochondrial pellet was incubated with Proteinase K (Roche, 3115828001) diluted as 1:2000 in the isolation buffer for 10 minutes on ice. Before adhering mitochondria to coverslips, the mitochondrial pellet was washed twice with the ice-cold isolation buffer.

Immunocytochemistry. Isolated mitochondria placed on prepared coverslips were incubated for 20 minutes to adhere mitochondria to coverslips, followed by the fixation using 1×PBS containing 4% paraformaldehyde and 0.3% glutaraldehyde for 15 minutes at room temperature. Coverslips were incubated with 1mg/ml $NaBH_4$ for 10 minutes to quench free amines. Fixed mitochondria were permeabilized with 1×PBS containing 0.3% triton-X for 10 minutes at room temperature, and blocked in 1×PBS containing 1% BSA and 0.05% sodium azide for 1 hour at room temperature. Coverslips were incubated with anti-FLAG antibody (Sigma, F7425) 1:500, anti-Myc antibody (Santa Cruz Biotechnologies, 9E10) 1:400, anti-TOMM20 antibody 1:200 (Abcam, ab56783), and anti-cytochrome C antibody 1:400 (BD Pharmingen Cat. 556433) diluted in the blocking solution at 4°C overnight. On the next day, coverslips were washed three times with PBST (0.1% TWEEN 20) for 10 minutes at room temperature. Secondary Alexa antibodies diluted as 1:400 in the blocking solution were incubated with coverslips for 2 hours at room temperature. After incubation, Coverslips were washed three times with PBST for 10 minutes at room temperature. Prolong Gold mounting reagent (Thermo Fisher Scientific, P36934) was used for mounting. For experiment to examine MCU processing by Calcium, 8 hours after transfection, HEK293 cells were incubated with 2μM ionomycin for 10 minutes, and immediately fixed by 4% paraformaldehyde. DIV 14 primary neurons were used for immunocytochemistry, followed by identical immunostaining procedure. In case of endogenous MCU staining, coverslips were incubated

with -20˚C methanol in the fixation step.

Co-immunoprecipitation and Western blotting. For Co-immunoprecipitation, 14 hours after transfection HEK293 cells were lysed using 400µl of RIPA buffer composed of 150mM NaCl, 50mM Tris-HCl, pH 7.4, 1% Triton-X, 0.1% SDS, 0.05% $C_{24}H_{39}NaO_4$ and protease inhibitor cocktail. After the Bradford assay (BioRad) was performed for measuring protein concentration, 1mg of proteins were incubated with 0.3µl of anti-Flag antibody (Sigma, F7425) or 1µl of anti-Myc antibody (Santa Cruz, 9E10) on rotator at 4°C overnight. On the next day, protein A/G agarose beads (ThermoFisher, #20421) were added to the protein-Ab mixtures, and incubated on rotator for at least 4 hours at 4°C. The Immunoprecipitated protein-bead complex was then washed with 1ml of the RIPA buffer, and centrifuged for 5 minutes at 5,000×g at 4°C. Supernatant after the centrifugation was then removed. After repeating the washing five times, Immunoprecipitated proteins are eluted with SDS loading dye by heating for 15 minutes at 95 °C.

For western blotting, SDS-PAGE gel composed of 4% stacking gel and 12% running gel was used to separate proteins. And these proteins were then transferred to a PVDF membrane (Millipore, #IPVH00010). Primary antibodies (Anti-Flag Ab; 1:3000, Anti-Myc Ab; 1:1000) diluted in 5% skim milk in 1×TBST (0.01% Tween 20) were incubated with the membrane at 4°C overnight. On the next day, the membrane was washed three times with 1×TBST for 10 minutes at room temperature, followed by the incubation with the secondary antibody diluted as 1:2500 in 5% skim milk in 1×TBST for 1 hour 30 minutes at room temperature. The membrane was then washed five times with 1×TBST for 10min at room temperature. ImageQuant LAS 4000 (GE Healthcare) was used for western blot imaging

Confocal Microscopy. Zeiss LSM 780 confocal microscope was used for all confocal images. For live image, a heating instrument was used for maintaining 37°C, and the Zeiss Definite Focus z-correction hardware was used for axial stability. A Plan-Apochromat 63×/1.4 oil immersion objective (Zeiss 420782-9900-000) was used for all immunocytochemistry images. For FRET experiment, Alexa 488 and Alexa 555 were used as the donor and acceptor, respectively. For isolated mitochondrial images, Individual mitochondrion was acceptor photo-bleached using a 561 nm laser over the course of 20 frames.

Calcium Measurements. N2A cells were transfected with the vectors of interest, R-GECO, and Mito-GEM-GECO, and incubated for at least 48 hours. For calcium measurement, a C-Apochromat 40x/1.2 Water Corr M27 objective (Zeiss 421767-9970-000) was used. Cells were imaged for at least 20 frames at 7 seconds intervals before and after treatment of 2µM ionomycin. R-GECO was used for confirming cytoplasmic calcium spike. For mitochondrial calcium measurement, blue-green emission ratiometric Mito-GEM-GECO was measured to calculate mitochondrial calcium level. All data was obtained from at least 3 experiments performed on cell passages and separate days. To calculate the relative calcium change, the calcium level before the treatment of 2µM ionomycin was considered as the initial value and baseline.

Velocity Measurements. Mitochondrial velocity in axons was calculated as described previously[40]. Mito-dendra2 plasmid vector was transfected into primary hippocampal neurons at DIV4. Experiments were performed at DIV13-17. One neuron per glass bottom dish was only subjected to live imaging. Each data was obtained from 2-5 independent primary neuron cultures. 405nm laser was used to make photo-converted mitochondria in cell body. Mitochondrial movement is observed using a Plan-Apochromat 20×/0.8 objective (Zeiss 420650-9901-000) in a 708μm × 708μm field of view for 1 hours at 15 seconds intervals. A kymograph was generated using data imported into Fiji software. MATLAB was used for generating a velocity distribution histogram. The histogram was fitted to a derived Fokker-Planck equation using Excel software. Real Stats Microsoft Excel plugin was used for Kolmogorov-Smirnov test.

Statistics. Dunnett's, Tukey's, and Fisher's LSD ANOVA, two-tailed Student's t-test, and paired Student's t-test were performed using Graphpad prism.

III. Results

1. MCU interacts with Miro1 through MCU's N-terminal domain.

In the previous publication from our group, we reported the mitochondrial matrix Ca^{2+} content regulated by MCU complex is critical for the mitochondrial mobility in axons[20]. Furthermore, we found Miro1 plays a key role in modulating Ca^{2+} uptake into the mitochondrial matrix[20]. These results suggest a possibility of functional coupling between MCU and Miro1 in a single complex. In order to test this possibility, Co-immunoprecipitation assay was performed using anti-Flag antibody or anti-Myc-antibody. We used plasmid vectors expressing MCU-Flag and Myc-Miro1 for the transfection into HEK293 cells (Figure 3A, B). And then, the co-transfected cells were collected and lysed by stringent RIPA buffer that allows these two mitochondrial membrane proteins, MCU and Miro1, to completely dissociate from the membranes[41]. As a result, we found MCU biochemically interacts with Miro1, and MCU was blotted at the position of 35kDa and 40kDa on a membrane (Figure 3C). Interestingly, we observed Miro1 has a significantly biased interaction with the upper 40kDa of MCU (Figure 3C). It is noted that MCU contains mitochondrial targeting sequence within its N-terminal domain subjected to a proteolytic cleavage following by the mitochondrial localization of MCU[21]. To further investigate whether Miro1 specifically interacts with MCU having N-terminal domain, we designed a vector expressing MCU mutant having deletion of N-terminal domain, MCU(Δ2-57a.a.) (Figure 3A). Co-immunoprecipitation assay using HEK293cells transfected with either MCU-Flag or MCU(Δ2-57a.a.)-Flag, and Myc-Miro1 was proceeded. The result obviously showed the deletion of the MCU's N-terminal domain abolishes its binding to Miro1 (Figure 3D). It suggests a possibility of new MCU's topology in mitochondrial membrane, in which MCU's N-terminus is projected toward the intermembrane space side of IMM. Next, to exclude the possibility that other regions of MCU are able to interact with Miro1, we selected mutation sites on the DIME motif of MCU because DIME motif is exposed to mitochondrial intermembrane space, forming the pore entrance[42]. Thus, we designed vectors expressing MCU mutants having alteration in several amino acids of the DIME motif, MCU(mutant1) and MCU(mutant2), for protein overexpression in HEK293 cells (Figure 3A). Co-immunoprecipitation assay was performed using HEK293 cell extracts with anti-Flag antibody. The result showed both MCU mutants still remain bound to Miro1, suggesting the DIME motif of MCU is not the region responsible for the interaction with Miro1 (Figure 3E). Furthermore, we tried to identify a region in Miro1 needed for the interaction with MCU. Expression vectors containing Miro1 without transmembrane domain, Miro1(ΔTM), or last 3a.a. beyond TM, Miro1(ΔKQR), were prepared for the transfection into HEK293cells (Figure 3B). The result of co-immunoprecipitation assay showed the deletion of Miro1's transmembrane domain eliminates the interaction between MCU and Miro1, while the deletion of 3 a.a. of Miro1 does not affect its binding to MCU (Figure 3F). It suggests the transmembrane domain of Miro1 is a key region required for the interaction with MCU.

Although co-immunoprecipitation assay is an appropriate method to verify physiologically relevant MCU-Miro1interaction, this assay, as *in vitro* biochemical methods, has difficulty to identify their interaction in intact mitochondria. Thus, we additionally performed FRET measurement by acceptor photobleaching with isolated mitochondria (Figure 3G). FRET efficiency of Flag-MCU and Myc-Miro1 was significantly higher than that of either Flag-MCU and TOMM20-Myc or Flag-MCU(Δ2-57a.a.) and Myc-Miro1, while Flag-MCU(mut1) having the mutation on DIME motif and Myc-Miro1 had similar level of FRET efficiency compared to that of Flag-MCU and Myc-Miro1 (Figure 3G). These results are consistent with the analysis of co-immunoprecipitation assay showing that Miro1 interacts with MCU through its N-terminal domain, not DIME motif. Together, these data indicate MCU and Miro1 exist in a single functional complex in mitochondria, and MCU's N-terminal domain is essential to the interaction between MCU and Miro1.

Figure 3. Interaction between MCU and Miro1. (A) Schematic representation of MCU domains and mutants. MCU proteins having the deletion of N-terminal domain (Δ2-57a.a.), or mutations on the DIME motif (^{257}EYSW^{260} to ^{257}AAAA^{260} or ^{261}DIME^{264} to ^{261}AAAA^{264}) are used for domain mapping. (B) Schematic representation of Miro1 domains and mutants. Miro1 proteins without 3a.a. (ΔKQR) or transmembrane domain (ΔTM) are used in mapping analysis. (C) Co-immunoprecipitation of MCU-Flag and Myc-Miro1. Protein extracts from MCU-Flag and Myc-Miro1 co-transfected HEK293 cells were immunoprecipitated by anti-Flag or Myc antibody conjugated with agarose A/G beads. The precipitate was subjected to western blotting with indicated antibodies. Interaction between MCU and Miro1 was observed. Interestingly, Myc-Miro1 preferentially binds to the unprocessed 40kDa band of MCU. (D) Co-immunoprecipitation of MCU(Δ2-57a.a.)-Flag and Myc-Miro1. Proteins produced from MCU(Δ2-57a.a.)-Flag expression vector was only detected on the processed 35kDa band of MCU. The binding to Myc-Miro1 was not observed. (E) Co-immunoprecipitation of Myc-Miro1 and MCU-Flag mutants. The interaction between MCU and Miro was not affected by mutations on the DIME motif (Mutant 1,2). (F) Co-immunoprecipitation of MCU-Flag and Myc-Miro1 mutants. Miro1 mutant having TM domain deletion (ΔTM) did not interact with MCU, while mutant Miro1 lacking 3a.a (ΔKQR) still remained bound to MCU. (G) FRET analysis of Flag-MCU and Myc-Miro1 in extracted mitochondria. FRET efficiency of Flag-MCU + Myc-Miro1 was significantly higher than that of Flag-MCU + TOMM20-Myc. Mutant on DIME motif (Mutant1) of MCU did not affect the binding to Miro1. The deletion of MCU's N-terminal domain (Δ2-57a.a.) significantly reduced the interaction between MCU and Miro1. Scale bar: 1μm. Tukey's box plot profile is shown. N= 72 mitochondria for Flag-MCU + TOMM20-Myc, 78 for Flag-MCU + Myc-Miro1 25 for Flag-MCU(mutant1) + Myc-Miro1, 23 for Flag-MCU(Δ2-57a.a.) + Myc-Miro1. $^{*}p<0.0001$.

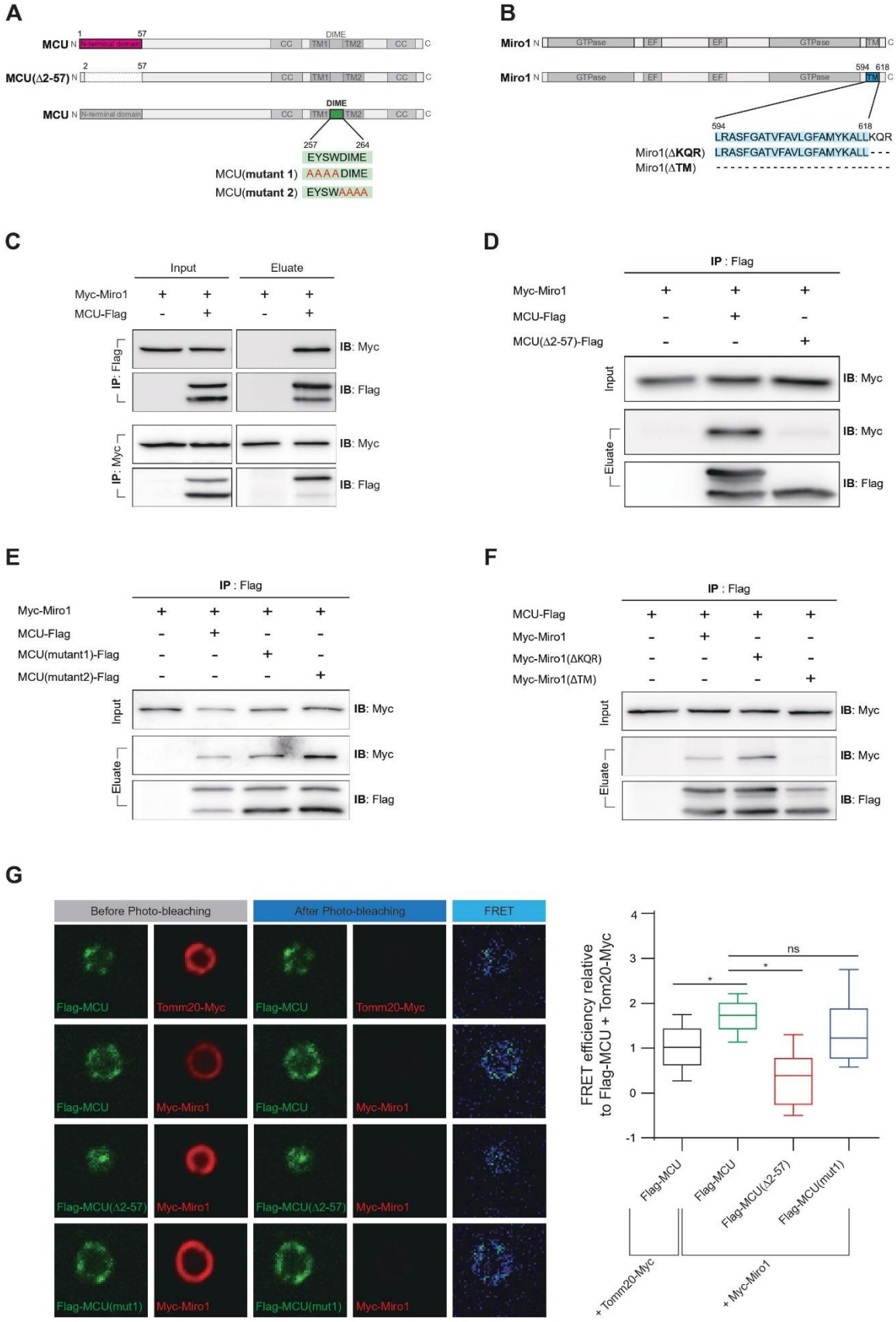

2. N-terminus of MCU has a transmembrane domain, which doesn't have a critical role in mitochondrial targeting signal.

Miro1's biased interaction with the N-terminal domain of MCU provided us with a question about roles of MCU's N-terminal domain in mitochondria. Previous research observed the molecular weight of MCU is lower than the predicted 40kDa[21], and is consistent with the predicted mitochondrial targeting sequence (p=0.976) in this domain which is proteolytically cleaved after mitochondrial localization[43]. However, the recently developed method for improved prediction of mitochondrial targeting sequence, MitoFates software, predicts non-presence of the mitochondrial targeting sequence in MCU's N-terminal domain because of lack of positively charged amphiphilicity α helix in the domain[44,45] (Figure 4A). Thus, we investigated whether this N-terminal domain indeed has a critical role in mitochondrial localization of MCU. To test this question, we cultured hippocampal primary neurons for co-transfection of either MCU-Flag or MCU(Δ2-57a.a.)-Flag and Myc-Miro1[46]. We found MCU mutant lacking the N-terminal domain and Myc-Miro1 are co-localized in axons in axons of primary neurons as well as MCU-Flag and Myc-Miro1, suggesting this domain is not required for targeting MCU into mitochondria. (Figure 4B). This result was further confirmed by using vectors expressing N-terminal domain of MCU coupled to superfolder GFP (sfGFP) and Mito-mCherry. The immunostaining analysis revealed MCU(1-57a.a.)-sfGFP and Mito-mCherry are not co-localized in axons of primary neurons, supporting N-terminal domain of MCU does not act as mitochondrial targeting sequence. (Figure 4B).

The next question is how MCU's N-terminal domain is interacts with Miro1, the outer mitochondrial membrane protein. Current putative topology of MCU has described both MCU's N and C-terminus are projected toward mitochondrial matrix[24], providing the low possibility of its binding to Miro1's transmembrane domain. However, the predictive analysis using TMBASE showed MCU's N-terminus has a potential transmembrane domain (18-38a.a.)[47], implying the possibility of new topology of unprocessed MCU with the data in Figure 3D. To explore this possibility experimentally, we prepared two vectors expressing Flag-tagged either N-terminus or C-terminus of MCU, and transfected these vectors with Myc-Miro1 into HEK293cells for comparison between staining patterns of Flag-MCU and that of MCU-Flag. We observed the Flag-MCU signal is overlapped with Myc-Miro1, a marker for the outer mitochondrial membrane. In contrast, the MCU-Flag signal is localized inside of Myc-Miro1 signal (Figure 4C). To better verify the topology of N-terminus of MCU, we isolated mitochondria from either Flag-MCU or MCU-Flag and Myc-Miro1 co-transfected HEK293 cells. The result showed more obvious difference than the data in Figure 4C, suggesting MCU's N-terminus is projected toward the outer mitochondrial membrane for the interaction with Miro1 (Figure 4D).

Then, a question is raised from results showing MCU's N-terminus projected toward the OMM and its binding to the transmembrane domain of Miro1 (Figure 3F). The question is whether N-terminus of MCU penetrates the OMM to reach Miro1's transmembrane domain. To solve this question, we

extracted mitochondria from HEK293 cells transfected with Flag-MCU and Mito-GFP, followed by treatment of proteinase K which selectively digests proteins or peptides projected toward the cytoplasmic side of the outer mitochondrial membrane. Proteinase K efficiently digested not only TOMM20, the outer mitochondrial membrane protein, but also Flag-tag at N-terminus of MCU. Whereas Intact mitochondria protected Mito-GFP, located inside the mitochondrial matrix, and cytochrome C, located within intermembrane space, from the digestion by proteinase K (Figure 4E), confirming MCU's N-terminus is able to extend out from the OMM and localized on the cytoplasmic side of this membrane. These results are consistent with the analysis using TMBASE that showed a predicted hydrophobic path (1-13a.a.) at the tip of MCU's N-terminus with the potential transmembrane domain (18-38a.a.) (Figure 4A). Together, these data revealed N-terminal domain of MCU is not required for its mitochondrial localization, and has a transmembrane domain, allowing it to interact with Miro1.

Figure 4. Identification of topology of N-terminus of MCU. (A) Schematic domain of MCU. The N-terminal domain of MCU involves a predicted hydrophobic patch (1-13a.a.) and transmembrane domain (18-38a.a.). (B) Immunostaining of Myc-Miro1 with MCU-Flag, MCU(Δ2-57a.a.)-Flag, or MCU(1-57a.a.)-sfGFP in axons of hippocampal primary neurons. MCU's N-terminal domain (1-57a.a.) is not sufficient to target MCU to mitochondria. Scale bar: 10μm. (C, D) Immunostaining of Flag-MCU or MCU-Flag with Myc-Miro1 in N2A cells and mitochondria isolated from HEK293 cells. The fluorescent signal of Flag-MCU, not MCU-Flag, is highly colocalized with that of Myc-Miro1. Scale bar: 1μm. (E) Proteinase K treatment in mitochondria isolated from Mito-GFP and Flag-MCU co-transfected HEK293 cells. The fluorescent signal of Flag-MCU and TOMM20 were disappeared by proteinase K treatment, while that of Cytochrome C and Mito-GFP was still shown. Scale bar: 1μm. Bar graph represents quantification of samples. N= 96 mitochondria for TOMM20 without proteinase K, 51 for TOMM20 with proteinase K, 43 for Cytochrome C without proteinase K, 82 for Cytochrome C with proteinase K.

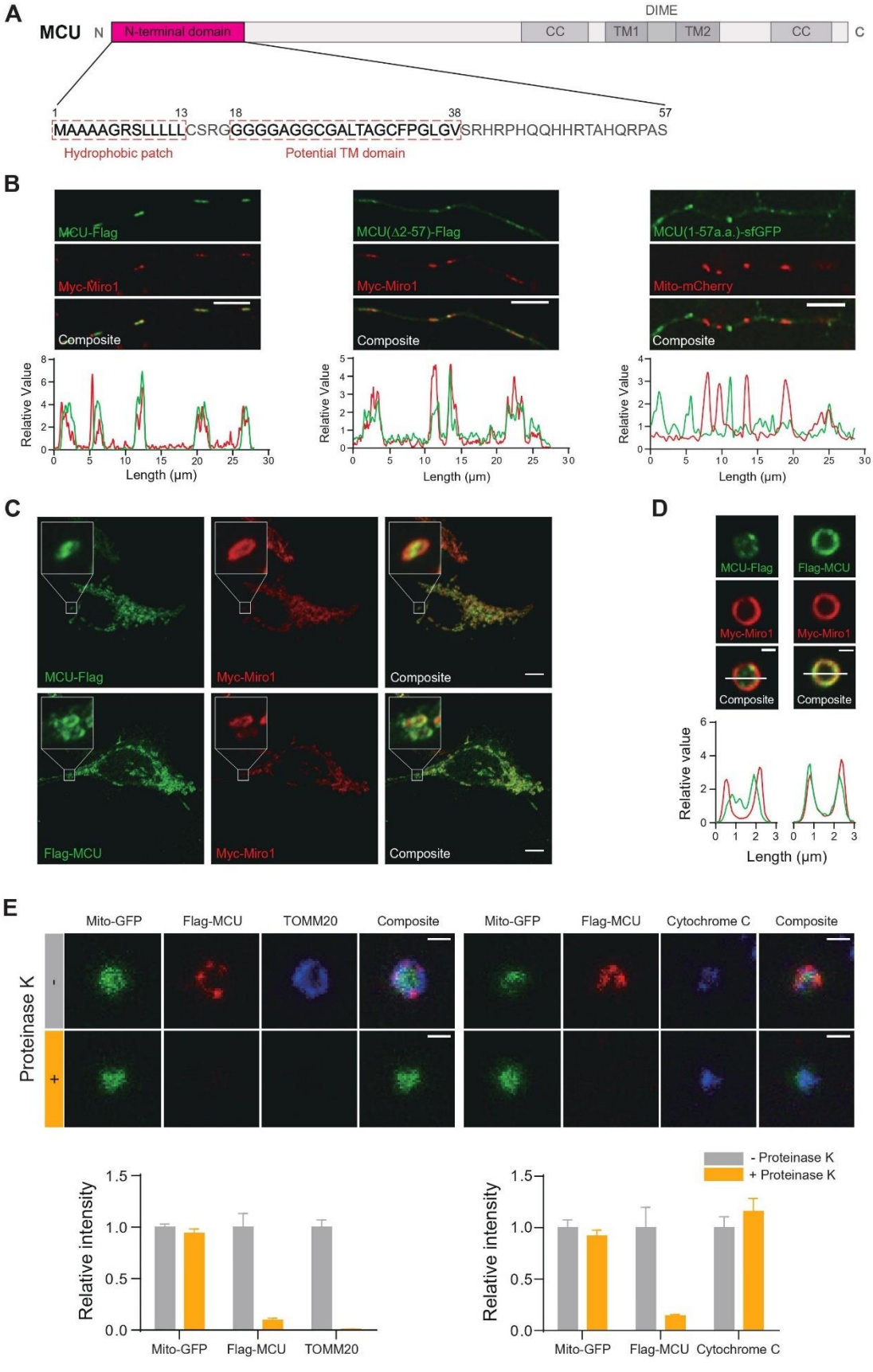

3. Intracellular Ca^{2+} elevation results in the cleavage of MCU's N-terminal domain.

MCU exists in two different forms, unprocessed MCU with the N-terminal domain, and processed MCU lacking this domain[21]. And we demonstrated the N-terminal domain of unprocessed MCU is able to interact with Miro1 within mitochondria. Then, we next asked which factors influence the interaction between MCU and Miro1. We hypothesized intracellular Ca^{2+} elevation triggers the cleavage of MCU's N-terminal domain, resulting in eliminating its interaction with Miro1. The reason why we choose Ca^{2+} is that it acts as a key molecule to regulate functions of both the MCU complex and Miro1 through binding to them[17]. To investigate this hypothesis, we designed a vector expressing Flag and sfGFP tagged at N-terminus and C-terminus of MCU, respectively. The location of these tags in Flag-MCU-sfGFP expressing HEK293 cells was investigated with and without treatment of 2μM ionomycin, a Ca^{2+} ionophore, for 10min[48]. Immunostaining Images showed both Flag and sfGFP signals are clearly colocalized within mitochondria without 2μM ionomycin treatment. However, Flag-tagged at MCU's N-terminus was distributed to the cytoplasm, while the sfGFP signal was still colocalized with mitochondria (Figure 5A). R^2 correlation analyzed from these images revealed a significant decrease in 2μM ionomycin treatment compared to DMSO treatment. It suggests the Ca^{2+} elevation stimulates the cleavage of N-terminal domain of MCU to disrupt the interaction between MCU and Miro1. Furthermore, we tried to confirm the cleavage of this domain through the western blotting. MCU-Flag expressed HEK293 cells were exposed to 2μM ionomycin before the steps for protein extraction. The result showed a decrease in the intensity of unprocessed MCU, and the ratio of unprocessed to processed MCU was also significantly decreased (Figure 5B).

Based on these results, we represented the MCU-Miro1 interaction model depicted in Figure 5C. In the model, MCU's N-terminal domain has the third transmembrane domain (TM3) that protrudes into the intermembrane space and hydrophobic patch to reach the Miro1's transmembrane domain, providing the new topology of MCU. Due to the new MCU topology, the interaction between MCU and Miro1 is maintained under a normal Ca^{2+} level. However, elevated intracellular Ca^{2+} initiates the cleavage of MCU's N-terminal domain, forming the previously established structure of MCU. This MCU structure does not allow it to interact with Miro1 (Figure 5C).

Figure 5. Cleavage of N-terminal domain of MCU by the elevated intracellular calcium. (A) Immunostaining of Flag-MCU-sfGFP after incubation with ionomycin in HEK293cells. Flag-tag and sfGFP were coupled to N-terminus and C-terminus of MCU, respectively. Flag-MCU-sfGFP transfected HEK293cells were incubated for 10min with 2μM ionomycin, followed by fixation. Scale bar: 5μm. The R^2 correlation between Flag and sfGFP was compared between paired samples with or without ionomycin treatment. N= 5 experiments. $^{*}p$= 0.0171. (B) Western blot data of MCU-Flag with ionomycin treatment. After 2μM ionomycin treatment, proteins were (*Figure legend continues.*)

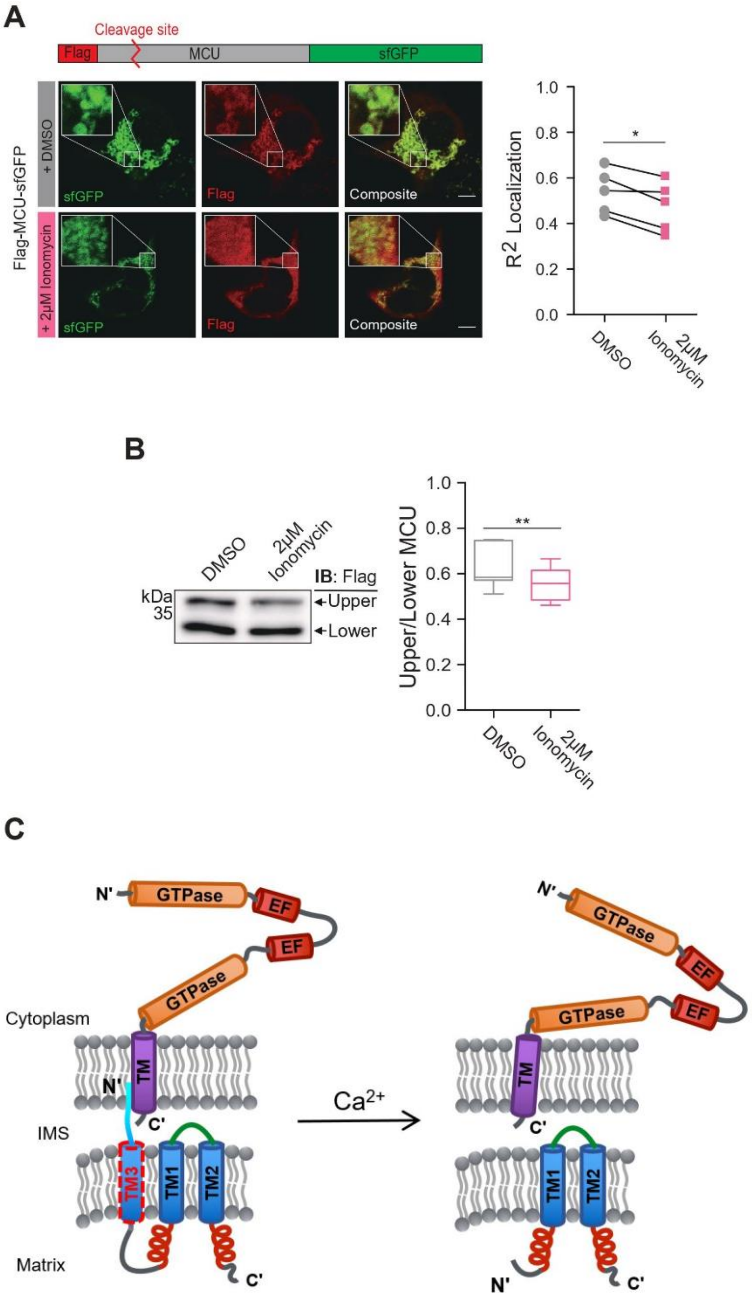

(*Figure legend continued.*) extracted from HEK293cells transfected with MCU-Flag, and then blotted with anti-Flag antibody. The ratio of unprocessed MCU (Upper band) to processed MCU (Lower band) is displayed as Tukey's boxplot profile. N= 7 experiments. $^{**}p$= 0.0094. (C) Model of MCU and Miro1. MCU's N-terminal domain has the third transmembrane domain that allow it to locate toward the cytoplasmic side of the outer mitochondrial membrane. Under the normal condition, cleavage of the N-terminus of MCU is not occurred, allowing it to maintain the interaction with the transmembrane domain of Miro1. However, intracellular Ca^{2+} elevation triggers the cleavage of N-terminal domain of MCU, resulting in loss of MCU-Miro1 interaction.

4. MCU-Miro1 interaction is essential for mitochondrial mobility in axons.

Having demonstrated that MCU and Miro exists in the single complex through the interaction between them, we next asked whether their interaction functionally regulates Ca^{2+} uptake through MCU and axonal mitochondrial movement by Miro1. To test this question, we designed a vector expressing MCU in which two consecutive amino acids in its N-terminus (R7A,S8A) were mutated because it is known that arginine, as a positively charged amino acid, acts as a gating charge carrier[49]. Interestingly, Co-immunoprecipitation assay with Myc-Miro1 revealed this mutant is present in the only 40kDa band of unprocessed MCU, and still interacts with Miro1 (Figure 6A). Thus, MCU(R7A,S8A)-Flag was also used to understand functional roles of MCU-Miro1 interaction.

To examine whether this interaction indeed modulate mitochondrial Ca^{2+} uptake through MCU complex. We used N2A cells transfected the genetically-encoded Ca^{2+} indicators (R-GECO and mito-GEM-GECO)[50], shMCU for knock-down of MCU, and either MCU-Flag or MCU mutants. Baseline of Ca^{2+} level was measured for at least 100sec before the addition of 2μM ionomycin. Intracellular Ca^{2+} elevation following treatment with ionomycin was confirmed by the cytoplasmic Ca^{2+} indicator, R-GECO. Mitochondrial Ca^{2+} level was monitored using the mitochondrial Ca^{2+} indicator, mito-GEM-GECO. As previously known[21,22]. We found MCU knock-down reduces mitochondrial Ca^{2+} uptake, and the mutation on DIME motif impairs the mitochondrial Ca^{2+} uptake. In contrast, Expression of MCU-Flag or MCU(Δ2-57a.a.)-Flag restored Ca^{2+} uptake reduced by MCU knock-down. We further found the expression of MCU(R7A,S8A)-Flag was not able to rescue Ca^{2+} influx to that of control (Figure 6B, C). Together, these data suggest the cleavage and dissociation of MCU's N-terminal domain from Miro1 is critical for the efficient Ca^{2+} uptake through MCU complex.

Next, we measured the number of mitochondria leaving cell body of neurons to understand a functional significance of the interaction in axonal mitochondrial movement. Both neurons expressing shMCU and MCU(Δ2-57a.a.)-Flag with shMCU showed a significantly decrease in the number of mitochondria leaving cell body compared to that of control and MCU-Flag with shMCU (Figure 6D), suggesting N-terminal domain of MCU interacting with Miro1 is essential for mitochondrial movement from cell body to axon. We also tested with neurons expressing MCU(R7A,S8A)-Flag with shMCU. The number of mitochondria leaving cell body in them was too small to measure enough mitochondrial mobility in axons (Figure 6D). It suggests this MCU mutant may act as a dominant-negative form that interrupts normal interaction between MCU and Miro1 to modulate the mitochondrial movement. To further analyze the mitochondrial movement regulated by MCU-Miro1 interaction, we used the kymograph analysis using a photo-switchable fluorescent protein, mito-dendra2, labeled mitochondria in axons[51] (Figure 6E). And, photoconverted mitochondria were only subjected to this analysis. Velocity distribution of mitochondrial movement was then fitted by a modified Fokker-Plank equation[40], providing improved representation of axonal mitochondrial mobility by eliminating bias toward axon areas with minimal movement activity. We found that MCU knock-down reduces the velocity of mobile

mitochondria in axon. The reduced velocity caused by MCU knock-down was restored by expression of MCU-Flag, while MCU(Δ2-57a.a.)-Flag cannot rescue the reduced mitochondrial velocity in axons (Figure 6F, G). Together, these results imply MCU-Miro1 interaction is critical for maintaining the axonal mitochondrial mobility; however, cleavage of MCU's N-terminus and elimination of this interaction result in an increase in stationary mitochondria in axons.

Figure 6. Axonal mitochondrial movement and Ca^{2+} influx capability altered by MCU-Miro1 interaction. (A) Co-immunoprecipitation of MCU(R7A,S8A)-Flag and Myc-Miro1. N-terminal domain of MCU(R7A,S8A)-Flag is not cleaved, and still interacts with Myc-Miro1. (B) Quantification of Ca^{2+} influx into mitochondria in N2A cells after 2μM ionomycin treatment. N2A cells were transfected with R-GECO and Mito-GEM-GECO as cytoplasmic and mitochondrial Ca^{2+} indicator, respectively. shCtrl, shMCU, shMCU + MCU-Flag, shMCU + MCU(Δ2-57a.a.)-Flag, or shMCU + MCU(R7A,S8A)-Flag were co-transfected with Ca^{2+} indicators. A single ANOVA test was applied to statistics. (C) Quantification of the Mito-GEM-GECP ratio at the first frame after exposing N2A cells to 2μM ionomycin. One-way ANOVA Dunnett's multiple-comparison test. Tukey's box plot profile is shown. N= 12 N2A cells for shCtrl, 12 for shMCU, 11 for shMCU + MCU-Flag, 12 for shMCU + MCU(Δ2-57a.a.)-Flag, 8 for shMCU + MCU(mut1)-Flag, 12 for shMCU + MCU(R7A,S8A)-Flag. $^{*}p<0.01$, $^{****}p<0.0001$. (D) The number of Mito-dendra photoconverted mitochondria leaving cell body per hour in hippocampal primary neurons. One-way ANOVA Dunnett's multiple-comparison test. Tukey's box plot profile is shown. N= 9 neurons for shCtrl, 12 for shMCU, 9 for shMCU + MCU-Flag, 5 for shMCU + MCU(Δ2-57a.a.)-Flag, 5 for shMCU + MCU(R7A,S8A)-Flag. $^{*}p<0.01$, $^{****}p<0.0001$. (E) Kymograph of axonal mitochondrial movement in hippocampal primary neurons. Mito-dendra labeled mitochondria in cell body were photoconverted to red color to allow tracking of mitochondria moving from the cell body toward the axon. Green colored mitochondria were already located in the axon. Images were acquired every 15 seconds for 1 hour. Horizontal scale bar: 50μm. Vertical scale bar: 10 minutes. (F) Velocity distribution of axonal mitochondria fitted to a derived Fokker-Planck equation. (G) Cumulative probability graph derived from the data in (F). Kolmogorov-Smirnov test was performed for determining statistical significance of *p*-value. $^{*}p<0.0002$.

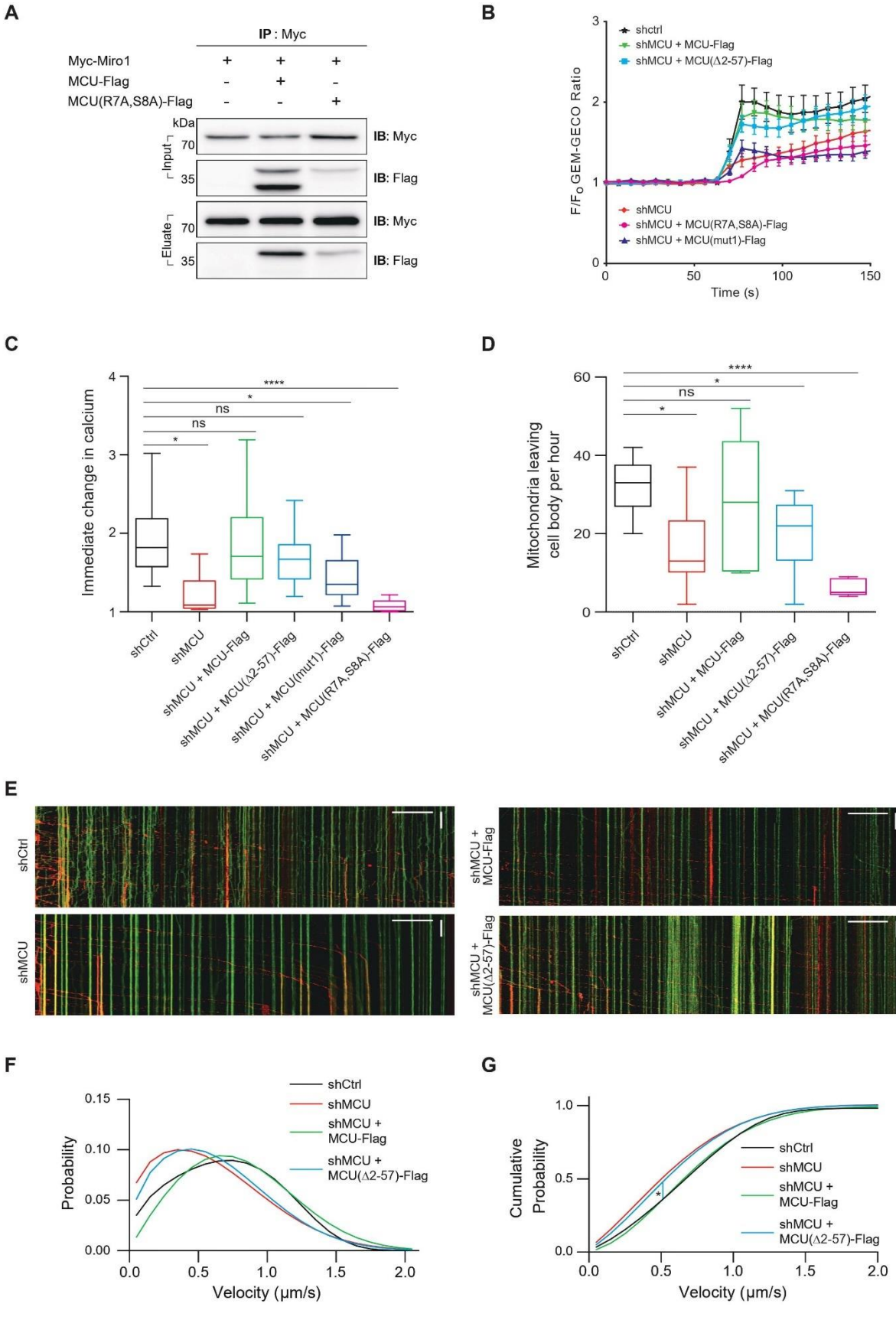

IV. Discussion

In this study, we discovered a novel MCU-Miro1 interaction. The N-terminal domain of MCU is a key region for interacting with Miro1, providing this domain with alternative functions that are different from a previously putative function as mitochondrial targeting sequence. We found this N-terminal domain is dispensable for targeting MCU to mitochondria. The interaction through the N-terminal domain rather proposes a model depicting new MCU topology within mitochondria. We also showed that dissociation of the interaction is caused by the cleavage of MCU's N-terminus in response to the intracellular Ca^{2+} elevation, and this cleavage is required for efficient Ca^{2+} uptake through MCU. We identified the MCU-Miro1 interaction is needed for efficient mitochondrial movement in axons.

Although we clearly observed the MCU and Miro1 interaction both biochemically and visually, there was a limitation that all evidences were demonstrated using the overexpression of MCU and Miro1 proteins. A critical issue in this study is whether the amount of endogenous MCU having N-terminal domain is enough to regulate the mitochondrial movement in the total amount of MCU. Unfortunately, we did not confirm clearly the interaction between endogenous MCU and Miro1, because the majority of MCU protein endogenously exists in the cleaved form lacking N-terminal domain[21]. However, a recent structural analysis of MCU revealed it forms a pore complex through the pentameric oligomerization[24], and our proposed model indicates that Miro1 is able to interaction with a single unprocessed MCU protein out of five in the complex, suggesting the low expression of unprocessed MCU is enough to regulate the mitochondrial transport. Moreover, mobile mitochondria become stationary as neurons mature, and eventually only 20-30% of mobile mitochondria are found in a typical neuron[20], that is consistent with a lowered presence of the unprocessed form of MCU.

Another issue is that while the interaction regulated by Ca^{2+} dependent cleavage is irreversible, mitochondrial mobility is reversible[52]. Given that neurons frequently respond to sudden changes in their internal and external signals, and mitochondria also rapidly sense and respond to their demand[53], our model may be required for rapid arrest of mitochondrial movement upon a high pulse of Ca^{2+}, and the resumption of mitochondrial movement may be compensated by other mitochondrial transport machineries.

In summary, we found the novel functional coupling between MCU and Miro1 to regulate mitochondrial Ca^{2+} uptake and transport in neurons, and demonstrated they share a molecular mechanism modulating these mitochondrial functions. It will be interesting for future studies to investigate enzymes and detailed mechanisms responsible for regulating MCU cleavage in response to the Ca^{2+} elevation. Also, our finding will help to understand dysfunctions of mitochondrial transport and Ca^{2+} influx shown in a variety of neurological disorders.

V. Reference

1 McBride, H. M., Neuspiel, M. & Wasiak, S. Mitochondria: more than just a powerhouse. *Curr Biol* **16**, R551-560, doi:10.1016/j.cub.2006.06.054 (2006).

2 L. Ernster, G. S. Mitochondria: a histroical review. *J Cell Biol* **91**, 227-255 (1981).

3 Williams, G. S., Boyman, L., Chikando, A. C., Khairallah, R. J. & Lederer, W. J. Mitochondrial calcium uptake. *Proc Natl Acad Sci U S A* **110**, 10479-10486, doi:10.1073/pnas.1300410110 (2013).

4 Hansford, R. G. Effect of micromolar concentrations of free Ca2+ ions on pyruvate dehydrogenase interconversion in intact rat heart mitochondria. *Biochemical Journal* **194**, 721-732, doi:10.1042/bj1940721 (1981).

5 G. Hajnoczky, L. D. R.-G., M.B. Seitz, A.P. Thomas. Decoding of cytosolic calcium oscillations in the mitochondria. *Cell* **82 (3)**, 415-424 (1995).

6 Murgia, M., Giorgi, C., Pinton, P. & Rizzuto, R. Controlling metabolism and cell death: at the heart of mitochondrial calcium signalling. *J Mol Cell Cardiol* **46**, 781-788, doi:10.1016/j.yjmcc.2009.03.003 (2009).

7 Myers, M. G., Jr. & Olson, D. P. Central nervous system control of metabolism. *Nature* **491**, 357-363, doi:10.1038/nature11705 (2012).

8 van Spronsen, M. *et al.* TRAK/Milton motor-adaptor proteins steer mitochondrial trafficking to axons and dendrites. *Neuron* **77**, 485-502, doi:10.1016/j.neuron.2012.11.027 (2013).

9 Johri, A. & Beal, M. F. Mitochondrial Dysfunction in Neurodegenerative Diseases. *Journal of Pharmacology and Experimental Therapeutics* **342**, 619-630, doi:10.1124/jpet.112.192138 (2012).

10 Mattson, M. P., Gleichmann, M. & Cheng, A. Mitochondria in neuroplasticity and neurological disorders. *Neuron* **60**, 748-766, doi:10.1016/j.neuron.2008.10.010 (2008).

11 Lin, M. T. & Beal, M. F. Mitochondrial dysfunction and oxidative stress in neurodegenerative diseases. *Nature* **443**, 787-795, doi:10.1038/nature05292 (2006).

12 Clapham, D. E. Calcium Signaling. *Cell* **80**, 259-268 (1995).

13 Augustine, G. J., Santamaria, F. & Tanaka, K. . Local Calcium Signaling in Neurons. *Neuron* **40**, 331-346 (2003).

14 Berridge, M. J. Neuronal Calcium Singnaling. *Neuron* **21**, 13-26 (1998).

15 Csordas, G. & Hajnoczky, G. SR/ER-mitochondrial local communication: calcium and ROS. *Biochim Biophys Acta* **1787**, 1352-1362, doi:10.1016/j.bbabio.2009.06.004 (2009).

16 Griffiths, E. J. & Rutter, G. A. Mitochondrial calcium as a key regulator of mitochondrial ATP production in mammalian cells. *Biochim Biophys Acta* **1787**, 1324-1333, doi:10.1016/j.bbabio.2009.01.019 (2009).

17 Niescier, R. F., Chang, K. T. & Min, K. T. Miro, MCU, and calcium: bridging our understanding of mitochondrial movement in axons. *Front Cell Neurosci* **7**, 148, doi:10.3389/fncel.2013.00148 (2013).

18 Giorgi, C., Marchi, S. & Pinton, P. The machineries, regulation and cellular functions of

mitochondrial calcium. *Nat Rev Mol Cell Biol* **19**, 713-730, doi:10.1038/s41580-018-0052-8 (2018).

19 Bang Wan, K. F. L., Joseph Y. Cheung, and Russell C. Scaduto, Jr. Regulation of Citric Acid Cycle by Calciu. *J Biol Chem* **264**, 13430-13439 (1989).

20 Chang, K. T., Niescier, R. F. & Min, K. T. Mitochondrial matrix Ca2+ as an intrinsic signal regulating mitochondrial motility in axons. *Proc Natl Acad Sci U S A* **108**, 15456-15461, doi:10.1073/pnas.1106862108 (2011).

21 Baughman, J. M. *et al.* Integrative genomics identifies MCU as an essential component of the mitochondrial calcium uniporter. *Nature* **476**, 341-345, doi:10.1038/nature10234 (2011).

22 De Stefani, D., Raffaello, A., Teardo, E., Szabo, I. & Rizzuto, R. A forty-kilodalton protein of the inner membrane is the mitochondrial calcium uniporter. *Nature* **476**, 336-340, doi:10.1038/nature10230 (2011).

23 Marchi, S. & Pinton, P. The mitochondrial calcium uniporter complex: molecular components, structure and physiopathological implications. *J Physiol* **592**, 829-839, doi:10.1113/jphysiol.2013.268235 (2014).

24 Oxenoid, K. *et al.* Architecture of the mitochondrial calcium uniporter. *Nature* **533**, 269-273, doi:10.1038/nature17656 (2016).

25 Raffaello, A. *et al.* The mitochondrial calcium uniporter is a multimer that can include a dominant-negative pore-forming subunit. *EMBO J* **32**, 2362-2376, doi:10.1038/emboj.2013.157 (2013).

26 Hoffman, N. E. *et al.* MICU1 motifs define mitochondrial calcium uniporter binding and activity. *Cell Rep* **5**, 1576-1588, doi:10.1016/j.celrep.2013.11.026 (2013).

27 Petrungaro, C. *et al.* The Ca(2+)-Dependent Release of the Mia40-Induced MICU1-MICU2 Dimer from MCU Regulates Mitochondrial Ca(2+) Uptake. *Cell Metab* **22**, 721-733, doi:10.1016/j.cmet.2015.08.019 (2015).

28 Plovanich, M. *et al.* MICU2, a paralog of MICU1, resides within the mitochondrial uniporter complex to regulate calcium handling. *PLoS One* **8**, e55785, doi:10.1371/journal.pone.0055785 (2013).

29 Sancak Y, M. A., Kitami T, Kovács-Bogdán E, Kamer KJ, Udeshi ND, Carr SA, Chaudhuri D, Clapham DE, Li AA, Calvo SE, Goldberger O, Mootha VK. EMRE Is an Essential Component of the Mitochondrial Calcium Uniporter Complex. *Science* **342**, 1379-1382 (2013).

30 Vais, H. *et al.* EMRE Is a Matrix Ca(2+) Sensor that Governs Gatekeeping of the Mitochondrial Ca(2+) Uniporter. *Cell Rep* **14**, 403-410, doi:10.1016/j.celrep.2015.12.054 (2016).

31 Chaudhuri, D., Artiga, D. J., Abiria, S. A. & Clapham, D. E. Mitochondrial calcium uniporter regulator 1 (MCUR1) regulates the calcium threshold for the mitochondrial permeability transition. *Proc Natl Acad Sci U S A* **113**, E1872-1880, doi:10.1073/pnas.1602264113 (2016).

32 Tomar, D. *et al.* MCUR1 Is a Scaffold Factor for the MCU Complex Function and Promotes Mitochondrial Bioenergetics. *Cell Rep* **15**, 1673-1685, doi:10.1016/j.celrep.2016.04.050 (2016).

33 Fransson, S., Ruusala, A. & Aspenstrom, P. The atypical Rho GTPases Miro-1 and Miro-2 have

essential roles in mitochondrial trafficking. *Biochem Biophys Res Commun* **344**, 500-510, doi:10.1016/j.bbrc.2006.03.163 (2006).

34 Devine, M. J., Birsa, N. & Kittler, J. T. Miro sculpts mitochondrial dynamics in neuronal health and disease. *Neurobiol Dis* **90**, 27-34, doi:10.1016/j.nbd.2015.12.008 (2016).

35 Tang, B. L. MIRO GTPases in Mitochondrial Transport, Homeostasis and Pathology. *Cells* **5**, doi:10.3390/cells5010001 (2015).

36 Sheng, Z. H. Mitochondrial trafficking and anchoring in neurons: New insight and implications. *J Cell Biol* **204**, 1087-1098, doi:10.1083/jcb.201312123 (2014).

37 Cai, Q. & Sheng, Z. H. Moving or stopping mitochondria: Miro as a traffic cop by sensing calcium. *Neuron* **61**, 493-496, doi:10.1016/j.neuron.2009.02.003 (2009).

38 Lopez-Domenech, G. *et al.* Loss of Dendritic Complexity Precedes Neurodegeneration in a Mouse Model with Disrupted Mitochondrial Distribution in Mature Dendrites. *Cell Rep* **17**, 317-327, doi:10.1016/j.celrep.2016.09.004 (2016).

39 Nguyen, T. T. *et al.* Loss of Miro1-directed mitochondrial movement results in a novel murine model for neuron disease. *Proc Natl Acad Sci U S A* **111**, E3631-3640, doi:10.1073/pnas.1402449111 (2014).

40 Niescier, R. F., Kwak, S. K., Joo, S. H., Chang, K. T. & Min, K. T. Dynamics of Mitochondrial Transport in Axons. *Front Cell Neurosci* **10**, 123, doi:10.3389/fncel.2016.00123 (2016).

41 Montserret R, M. M., Böckmann A, Geourjon C, Penin F. Involvement of electrostatic interactions in the mechanism of peptide folding induced by sodium dodecyl sulfate binding. *Biochemistry* **39**, 8362-8373 (2000).

42 Baradaran, R., Wang, C., Siliciano, A. F. & Long, S. B. Cryo-EM structures of fungal and metazoan mitochondrial calcium uniporters. *Nature* **559**, 580-584, doi:10.1038/s41586-018-0331-8 (2018).

43 Claros MG, V. P. Computational method to predict mitochondrially imported proteins and their targeting sequences. *Eur J Biochem* **241**, 779-786 (1996).

44 Fukasawa, Y. *et al.* MitoFates: improved prediction of mitochondrial targeting sequences and their cleavage sites. *Mol Cell Proteomics* **14**, 1113-1126, doi:10.1074/mcp.M114.043083 (2015).

45 G, v. H. Mitochondrial targeting sequences may form amphiphilic helices. *EMBO J* **5**, 1335-1342 (1986).

46 Martell, J. D. *et al.* Engineered ascorbate peroxidase as a genetically encoded reporter for electron microscopy. *Nat Biotechnol* **30**, 1143-1148, doi:10.1038/nbt.2375 (2012).

47 Hofmann, K. TMbase-a database of membrane spanning proteins segments. *Biol. Chem. Hoppe-Seyler* **374**, 166 (1993).

48 Mallilankaraman, K. *et al.* MCUR1 is an essential component of mitochondrial Ca2+ uptake that regulates cellular metabolism. *Nat Cell Biol* **14**, 1336-1343, doi:10.1038/ncb2622 (2012).

49 Hristova, K. & Wimley, W. C. A look at arginine in membranes. *J Membr Biol* **239**, 49-56, doi:10.1007/s00232-010-9323-9 (2011).

50 Zhao Y, A. S., Wu J, Teramoto T, Chang YF, Nakano M, Abdelfattah AS, Fujiwara M, Ishihara T, Nagai T, Campbell RE. An expanded palette of genetically encoded Ca2+ indicators. *Science* **333**, 1888-1891 (2011).

51 Chudakov, D. M., Lukyanov, S. & Lukyanov, K. A. Tracking intracellular protein movements using photoswitchable fluorescent proteins PS-CFP2 and Dendra2. *Nat Protoc* **2**, 2024-2032, doi:10.1038/nprot.2007.291 (2007).

52 Saotome, M. *et al.* Bidirectional Ca²⁺-dependent control of mitochondrial dynamics by the Miro GTPase. *Proceedings of the National Academy of Sciences* **105**, 20728-20733, doi:10.1073/pnas.0808953105 (2008).

53 Cheng, A. *et al.* Mitochondrial SIRT3 Mediates Adaptive Responses of Neurons to Exercise and Metabolic and Excitatory Challenges. *Cell Metab* **23**, 128-142, doi:10.1016/j.cmet.2015.10.013 (2016).

VI. Acknowledgement

I would like to express my sincere appreciation to my supervisor, Prof. Kyung Tai Min, for his advice, instruction, and motivation during my graduate school years. I will never forget a lot of lessons from his experimental experience and his life as a true scientist. I convince that his teaching and wisdom will surely help my future life and career. Also, I would like to express sincere thanks to my thesis examining committee, professor Byoung Heon Kang and professor Chan Young Park.

Next, I would like to express my sincere gratitude to MinLab members for their support and advice related to my research. Firstly, I am thankful for Dong Keun Park. I learned many basic experimental skills and how to design experimental procedures while assisting him. Thanks to So Yeon Lee, I was able to easily proceed several experiments using cultured primary neurons. And she gave me precise knowledge based on her experience to reduce unnecessary experiments and waste of time. Also, I am thankful for Chi Yeol Choi. He gave me a lot of advice and encouragement to develop my experiments and research. I believe he will complete his course soon and become a better researcher. I want to thank to Jong Min Park and Young Im Yu. I was able to run many experiments without delay due to their accurate and careful mouse management. I hope them to finish their course and research successfully. I am also grateful to Ji Won Park and Hye Rin Kim. They actively participated and involved in laboratory work than anyone else. I believe that a bright future will await them. I wish all good luck in future of MinLab members.

Finally, I should like to express my deepest gratitude to my family and friends. My family always support and encourage me in any situation. They listened carefully and respected my decision. Also, my friends gave me the courage and faith to do well when I had a hard time.